

AD-A066 760

NAVY ELECTRONICS LAB SAN DIEGO CALIF
APPLICATION OF COMPUTER TECHNIQUES TO THE PREDICTION OF UNDERWA--ETC(U)
1956 E R ANDERSON, M A PEDERSEN

F/G 20/1

UNCLASSIFIED

NL

1 OF 1
ADA
066760



END
DATE
FILMED
5 79
DDC

UNCLASSIFIED

Anderson and Pedersen

Downgraded at 3-year intervals; Declassified after 12 years.

automatic-downgrading statement (first page only)

type security here

start here for all pages after the first

12 32p.

LEVEL II

11 1956

MOST Project 3

on first page type title of paper here

6 APPLICATION OF COMPUTER TECHNIQUES TO THE PREDICTION OF UNDERWATER SOUND PROPAGATION

author affiliation city, state

10 E. R. Anderson M. A. Pedersen U. S. Navy Electronics Laboratory San Diego, California

The efficient use of the Navy's increasingly complex sonar

first line of paper

In recent years the U. S. Navy has... into operational use increasingly complex sonar systems. The efficient use of these systems depends on a detailed knowledge of the behavior of the acoustic energy contained in the underwater acoustic paths which they employ. Once the behavior of the acoustic energy is understood then operational prediction in terms of equipment and environmental parameters becomes possible.

In trying to obtain

At NEL a great deal of research effort has been devoted to obtaining an objective understanding of the nature of the propagation of acoustic energy in the convergence zone and the surface channel paths. As this understanding has grown more and more effort has been devoted to the prediction of intensity fields. Since the propagation of energy in the convergence zone and surface channel paths is a complex phenomena involving both acoustic and environmental parameters, this effort would not have attained the success it has without access to and utilization of modern computer facilities and techniques. This report discusses: (1)

This presentation will consist of three parts: (1) a discussion of an acoustic intensity program for estimating convergence zone propagation loss using ray theory; (2) a discussion of an acoustic intensity program for estimating propagation loss associated with surface channels using normal mode theory; and (3) a discussion of work at NEL on summarizing information on the oceanographic variables pertinent to these intensity computations.

RAY THEORY ACOUSTIC INTENSITY PROGRAM. The input to the convergence zone propagation loss program is point temperature and salinity data taken from the surface to the bottom and the output is the propagation loss as a function of horizontal distance and depth for a given source depth.

AD AO 66760

DDC FILE COPY

DDC REPORT R 100116 APR 2 1979 F loss

DISTRIBUTION STATEMENT A Approved for public release; Distribution Unlimited

UNCLASSIFIED

CONFIDENTIAL

type security class here

type page no. here

ENCL. 4

253 550

LB

UNCLASSIFIED

Anderson and Pedersen

type security classification here **CONFIDENTIAL**

White Section	<input checked="" type="checkbox"/>
Red Section	<input type="checkbox"/>
AK LATER	
AN FILE	
DISTRIBUTION/AVAILABILITY CODES	
Public-reading room	
Document	
Page	
(only)	
A	

start here for all pages after the first

on first page type title of paper here

author affiliation city, state

first line of paper

The computer program complex consists of the six sub-programs listed on slide 1. The first program computes the sound velocity from pressure, temperature, and salinity after first converting depth to pressure. The second program modifies the velocity-depth data points to correct for the curvature of the earth. The third program divides the transformed profile into layers and fits an analytic function to each layer such that the velocities and their first depth derivatives are continuous at the layer interfaces. The fourth program computes ranges, intensities, and travel times using ray theory for surface-reflected, purely refracted, and bottom reflected rays assuming a flat bottom. The fifth program processes all the data computed in the fourth program for a given combination of source and receiver depths. It interpolates, sums the intensities assuming random phase, converts to decibel loss, and adds in attenuation with the final output being the propagation loss for 100-yard range increments for each selected receiver depth. It also edits the data for plotting purposes. The sixth program plots enough points to define the propagation loss contours. These six programs consist of about 13500 commands and constants.

This computation provides a wealth of data on propagation loss that can be presented in many ways. Slide 2 shows a detailed summary of the results of one computation for a 6000-foot source depth. Propagation loss as a function of range and depth is contoured for 5 db intervals. The degree of detail is obvious from the complexity of the contouring. Slide 3 is a simplified presentation of the same data prepared for a specific purpose. Only one loss contour is shown. The shaded area shows where the propagation loss is less than 100 db and the unshaded greater than 100 db. Additional presentations can be prepared from the basic computations depending upon the acoustic problem under consideration. The important point, however, is that the computation results in a degree of objective detail heretofore unavailable. This detail is then available for many specific uses.

The preceding discussion has been entirely theoretical and one might reasonably ask how well the theoretical results agree with experimental observation. Slide 4 compares experimental and theoretical results for an acoustic experiment conducted off San Diego in January 1955. The sound velocity profile was obtained from measurement of temperature, salinity, and depth made during the experiment. In this experiment the source depth was 385 feet, the receiver depth 400 feet, and the frequency 530 cps. The irregular line connects the experimental data points and the solid line shows the theoretical calculations. Range in nautical miles is shown on the abscissa and propagation loss in decibels on the ordinate. The two figures are continuous in range. Many additional experimental and theoretical comparisons have been made for a variety of oceanographic and acoustic situations with results similar to those shown in this slide.

UNCLASSIFIED

CONFIDENTIAL

type security class here

leave blank

type page no. here

UNCLASSIFIED

Anderson and Pedersen

~~CONFIDENTIAL~~

automatic-
downgrading
statement
(first page
only)

start here
for all
pages after
the first

Those of you familiar with previous attempts to objectively describe the acoustic intensity field will recognize that this computational procedure represents a real advance in understanding the behavior of acoustic energy being propagated in the convergence zone path.

on first
page type
title of
paper here

NORMAL MODE ACOUSTIC INTENSITY PROGRAM. The second computer program complex that has been developed at NEL is based on normal mode, rather than ray theory, and deals with the problem of computing the propagation loss in surface sound channel paths. One of the important features of normal mode theory is that propagation loss can be calculated to any range for sources and receivers below the layer as well as in the layer. In other words, there are no shadow zones in the computed intensity field based on normal mode theory as there are in ray theory.

author
affiliation
city, state

The model for this computation is a bi-linear duct consisting of one layer of water having a linear sound velocity distribution overlying a second layer containing a different linear distribution of velocity. The inputs are depth and sound velocity gradient in the first layer, gradient in the second layer, and absolute value of the surface sound velocity. The output is a plot of contoured propagation loss as a function of range and depth for a given source depth and frequency.

first line
of paper

The method is an extension of the theory treated by Furry and Marsh. Early work by these and other investigators was limited because of computational difficulties which required gross mathematical approximations. These approximations limited the accuracy and applicability of the theory to a marked degree. Utilizing digital computers it is possible to avoid these approximations. This problem involves computations in the complex plane and consists of about 6000 commands and constants. Those of you acquainted with normal mode theory and its applications are certainly well aware of the mathematical complications associated with numerical applications of the theory.

Slide 5 is a sample of the output from this program. Contoured plots come directly off the on-line high speed printer and on a CDC 1604 computer take about two minutes to produce. Range in kiloyards is shown on the abscissa, depth in feet on the ordinate, and propagation loss contoured for 10 db intervals. The inputs for this computation are surface velocity 4920 feet per second, sound channel depth 100 feet, sound channel gradient 1.8 feet per second per 100 feet, gradient below the channel 33.3 feet per second per 100 feet, frequency 1.2 kilocycles, and source depth 15 feet. This is typical of a simple acoustic field. Slide 6 is a plot obtained by changing the layer depth to 300 feet and leaving the other variables the same as for the previous computation. It is typical of a complex acoustic field. By varying the six inputs many different fields, exhibiting all degrees of complexity, are obtained.

type secur-
ity class
here

~~CONFIDENTIAL~~

UNCLASSIFIED 3

leave blank

type page
no. here

Opt. author, test, pub. date

type security classification here ~~CONFIDENTIAL~~

automatic-downgrading statement (first page only)

start here for all pages after the first

on first page type title of paper here

author affiliation city, state

first line of paper

Again one might ask how well these theoretical computations agree with experimental observation. Slide 7 summarizes results from an experiment conducted off the California coast. In this test the surface channel was 300 feet deep, the source depth 55 feet, the receiver depth 50 feet, and frequency 530 cps. The dots show the experimental data. The solid line is the theoretical calculation based on environmental factors measured at the source ship, while the dashed line is based on environmental factors measured at the receiving ship. Agreement between theory and experiment is quite good as far as the general level of propagation losses is concerned. Note the beat patterns that appear in both the experimental and theoretical losses. These are caused by the interaction between normal modes.

Slide 8 is another comparison from the same data but for a 400-foot receiver located about 100 feet below the surface channel. The experimental data drops below noise between 14 and 15 miles and beyond 17 miles. At 15 miles the experimental loss is some 25 db greater than for the 50-foot receiver shown in the previous slide. Note that normal mode theory predicts this large difference in levels between in-layer and below-layer receivers and also predicts about the proper decay with range. This contrasts markedly with ray theory which predicts a shadow zone beyond 3 miles. This ability to utilize the more exact normal mode theory, in place of ray theory, makes it possible to obtain much more realistic computed propagation loss fields.

ESTIMATION OF ENVIRONMENTAL PARAMETERS. The two computer program complexes just discussed define the environmental parameters for which information is necessary in order to obtain realistic propagation loss information for the convergence zone and surface channel acoustic paths.

In the National Oceanographic Data Center are archived many millions of oceanic temperature and salinity measurements made over the years for a variety of purposes. This data collection is the basic oceanographic data collection for obtaining the required input information. During the past few years the Oceanometrics Group at NEL has been attempting to develop techniques and methods of summarizing oceanographic information required by the Navy's acoustic program. To illustrate this work I would like to review the results of two studies.

The first study deals with the problem of summarizing sea-surface temperature observations. Historically such data have been summarized by averaging over arbitrary size areas and time intervals and the resulting averages plotted and subjectively contoured. At NEL an attempt is being made to approach this problem from a more objective point of view utilizing regression analysis concepts. Although regression techniques were developed many decades ago they have rarely been used by oceanographers because of the complexity inherent in developing realistic models and the magnitude of the

~~CONFIDENTIAL~~

type security class here

leave blank

4 type page no. here

type security classification here

~~CONFIDENTIAL~~

automatic-downgrading statement (first page only)

start here for all pages after the first

arithmetic task required to evaluate the necessary constants. With the recent progress in computer development the arithmetic difficulties are being solved with the result that it is now practical to use complex models.

on first page type title of paper here

I would like to present the results of one such analysis of sea-surface temperature measurements made in the four one-degree latitude strips shown in slide 9. The measurements made in these four strips were treated as a single sample drawn from the area 30° to 49° N and extending seaward about 700 miles and for an 18-month time interval extending from 1 April 1949 to 1 October 1950. The total number of observations in each strip and their distribution in time and space are also shown in the slide. In the shaded areas one to twenty observations were made and in the unshaded areas no observations were made.

author affiliation city, state

Slide 10 shows the regression equation that was fitted to the observed data. Three main effects -- latitude, longitude, and day-of-year -- and three interactions -- latitude by day, longitude by day, and latitude by longitude -- were considered. This resulted in a 22-variable equation with 23 constants to be determined by least squares.

first line of paper

Slide 11 summarizes the statistical results of the analysis. The number of observations was 807, the per cent of variance explained by regression was 85.7 per cent, the multiple correlation coefficient was 0.93, and the standard deviation of the observations about regression was 1.9°F.

Slide 12 shows the location in time and space of 971 temperature observations made in this area during fiscal year 1950. These observations were not used in obtaining the regression equation but were used as a control to see how well the regression equation could estimate independently observed sea-surface temperatures. The difference between the observed temperature and that computed from the regression equation was obtained and the results are shown in the form of a histogram in slide 13. The standard deviation of the differences was 2.3°F compared to 1.9°F for the regression equation. The close agreement certainly suggests that the two sets of data are drawn from the same population.

Slide 14 shows a sea-surface temperature chart for 8 November 1950 contoured from temperatures obtained from the regression equation. It is noted that the regression equation faithfully portrays the main oceanographic feature, namely, the tongue of cold water that is the result of upwelling occurring along the coast.

The second study I would like to review is concerned with the shape of the vertical sound velocity profile. This study was based on an examination of approximately 1000 hydrographic casts made in the North Pacific north of 20° N in 1955. All data were

type security class here

type security classification here **CONFIDENTIAL**

automatic downgrading statement (first page only)

start here for all pages after the first

taken during the summer and are essentially time independent. Each set of hydrographic cast data was converted into sound velocity and plotted as a function of depth. A study of these plotted data suggested three major types which were categorized as type A single minimum, type B double thermocline, and type C double minimum.

on first page type title of paper here

Slide 15 shows the four single minimum sub-types. Sub-type 1 and sub-type 2 have a single minimum at about 100 meters with sub-type 1 having a minimum velocity less than 4800 feet per second and sub-type 2 having a minimum velocity greater than 4800 feet per second. Sub-type 3 has a minimum at about 500 meters and sub-type 4 a broad, almost isovelocity, minimum deeper than 750 meters and sometimes as deep as 1200 meters.

author affiliation city, state

Slide 16 shows the two double thermocline sub-types. Both sub-types exhibit a near surface shallow thermocline with a deeper thermocline at about 200 meters in the case of sub-type 5 and at about 400 meters in the case of sub-type 6.

first line of paper

Slide 17 shows the three double minimum sub-types. In sub-type 7 both minima are shallow with the shallowest minimum having the lowest velocity, in sub-type 8 both minima are deeper with the deeper minimum having the lower velocity, and in sub-type 9 the minima are still deeper with the deepest minimum having a much lower velocity than the shallower minimum.

After identifying these nine basic shapes each of the 1000 profiles were compared with the shapes and classified as to sub-type. If a profile shape was different from these nine basic shapes it was classified as transitional.

Next the shape numbers were plotted on a locator map to see whether or not large volumes could be identified as having the same shape. The results are summarized in slide 18. Profiles taken in the white areas were of the indicated sub-type. Gray areas contain transitional profiles. There are three major transitional areas -- one off the west coast of North America, associated with the California Current; a second in the western Pacific associated with the westward drift; and a third off Japan where there is an admixture of warm water from the Kuroshio Current and cold water from the Sea of Okhotsk. Thus this portion of the North Pacific contains eight large homogeneous volumes and three transitional volumes.

To illustrate what is meant by the terms "transitional volume" and "homogeneous volume" I would like to show two sections of profiles. Slide 19 shows the location of a section taken in a homogeneous area. This 600-mile section is located in the sub-type 9 volume with one profile taken in the sub-type 6 volume. Slide 20 shows the individual profiles. The area to the left of the 4900 feet per second value of velocity is shaded. The almost exact

type security class here

type security classification here ~~CONFIDENTIAL~~

automatic-downgrading statement (first page only)

start here for all pages after the first

taken during the summer and are essentially time independent. Each set of hydrographic cast data was converted into sound velocity and plotted as a function of depth. A study of these plotted data suggested three major types which were categorized as type A single minimum, type B double thermocline, and type C double minimum.

on first page type title of paper here

Slide 15 shows the four single minimum sub-types. Sub-type 1 and sub-type 2 have a single minimum at about 100 meters with sub-type 1 having a minimum velocity less than 4800 feet per second and sub-type 2 having a minimum velocity greater than 4800 feet per second. Sub-type 3 has a minimum at about 500 meters and sub-type 4 a broad, almost isovelocity, minimum deeper than 750 meters and sometimes as deep as 1200 meters.

author affiliation city, state

Slide 16 shows the two double thermocline sub-types. Both sub-types exhibit a near surface shallow thermocline with a deeper thermocline at about 200 meters in the case of sub-type 5 and at about 400 meters in the case of sub-type 6.

first line of paper

Slide 17 shows the three double minimum sub-types. In sub-type 7 both minima are shallow with the shallowest minimum having the lowest velocity, in sub-type 8 both minima are deeper with the deeper minimum having the lower velocity, and in sub-type 9 the minima are still deeper with the deepest minimum having a much lower velocity than the shallower minimum.

After identifying these nine basic shapes each of the 1000 profiles were compared with the shapes and classified as to sub-type. If a profile shape was different from these nine basic shapes it was classified as transitional.

Next the shape numbers were plotted on a locator map to see whether or not large volumes could be identified as having the same shape. The results are summarized in slide 18. Profiles taken in the white areas were of the indicated sub-type. Gray areas contain transitional profiles. There are three major transitional areas -- one off the west coast of North America, associated with the California Current; a second in the western Pacific associated with the westward drift; and a third off Japan where there is an admixture of warm water from the Kuroshio Current and cold water from the Sea of Okhotsk. Thus this portion of the North Pacific contains eight large homogeneous volumes and three transitional volumes.

To illustrate what is meant by the terms "transitional volume" and "homogeneous volume" I would like to show two sections of profiles. Slide 19 shows the location of a section taken in a homogeneous area. This 600-mile section is located in the sub-type 9 volume with one profile taken in the sub-type 6 volume. Slide 20 shows the individual profiles. The area to the left of the 4900 feet per second value of velocity is shaded. The almost exact

type security class here

~~CONFIDENTIAL~~

leave blank

640508 0627

6 type page no. here

type security classification here ~~CONFIDENTIAL~~

automatic-downgrading statement (first page only)

start here for all pages after the first

similarity in shape over distances of hundreds of miles is quite obvious.

on first page type title of paper here

Slide 21 shows the location of a 300-mile section located in the transitional volume off the coast of Japan. The upper portion of slide 22 shows the profiles over northern half of the section. These shapes exhibit relatively small shape changes. The lower portion shows the profiles for the southern half of the section and illustrates marked changes in profile shape occurring over distances of 20 to 40 miles -- approximate convergence zone distances.

author affiliation city, state

This analysis suggests three implications -- to operations it implies that in the homogeneous areas acoustic performance should be stable and predictable while in the transition areas it should be variable and less predictable; to research it suggests that acoustic experiments should be conducted in the different profile volumes and the transitional volumes before generalizations are attempted; and to survey programs such analyses gives guidance as to areas that should be surveyed.

first line of paper

PREDICTION OF ACOUSTIC PERFORMANCE. In the discussion so far information explaining acoustic results by means of theoretical calculations based on oceanographic data taken during acoustic tests in familiar waters has been presented. Our current ability to predict the acoustic field in areas significantly different from NEL's customary test areas is suggested by slide 23. Convergence zone echo-ranging experiments were conducted at two locations -- area 1, located in a transition region 300 miles west of Vancouver Island and, area 2, located in the homogeneous region 100 miles south of Kodiak. In laboratory preparation for these tests, appropriate oceanographic stations were examined and sound velocity profiles forecast for the two areas. Predicted propagation losses were calculated for each of these areas. Three horizontal bars are shown for each area. The upper bar shows the range interval at the first convergence zone over which echoes were experimentally observed, the next bar the expected interval calculated by using a sound velocity profile obtained from measurements made concurrent with the acoustic experiments, and the lower bar the predicted interval obtained from a predicted sound velocity profile. Range prediction obtained from the predicted sound velocity profiles was not as good in the transitional volume, area 1, as in the homogeneous volume, area 2, presumably because of large horizontal variation in profile shape. However, in both instances the agreement between the predicted detection range and the observed detection range is quite remarkable attesting to the validity of the prediction approach.

I would like to conclude with a comment on the possibility of developing an operational acoustic performance prediction technique based upon the research I have just discussed. From what has been accomplished so far it seems well within the realm of possibility to develop a system for predicting the sound velocity distribu-

type security class here

~~CONFIDENTIAL~~

type page no.

type author's last name here

Anderson and Pedersen

type security classification here ~~CONFIDENTIAL~~

automatic-downgrading statement (first page only)

start here for all pages after the first

tion and its influence on various acoustic parameters, from periods of a few days to a few tens of days; as well as to give the oceanometric expectations for any time period in the future. It is not very difficult to visualize a shipboard equipment where the analyzed historical oceanographic data and sonar equipment parameters have been stored; observations taken during the preceding few days or weeks introduced; and by entering the latitude, longitude, and time-of-year obtaining a predicted acoustic field.

on first page type title of paper here

author affiliation city, state

first line of paper

type security class here

leave blank

640508 C627

8

type page no. here

**RAY THEORY ACOUSTIC INTENSITY
COMPUTATIONAL PROGRAM**

Sub-Program

1. Sound Velocity
2. Curved Earth Simulation
3. Curve Fitting
4. Acoustic Intensity
5. Propagation Loss Computation
6. Propagation Loss Plotting

Figure 1

640508 C627

~~CONFIDENTIAL~~

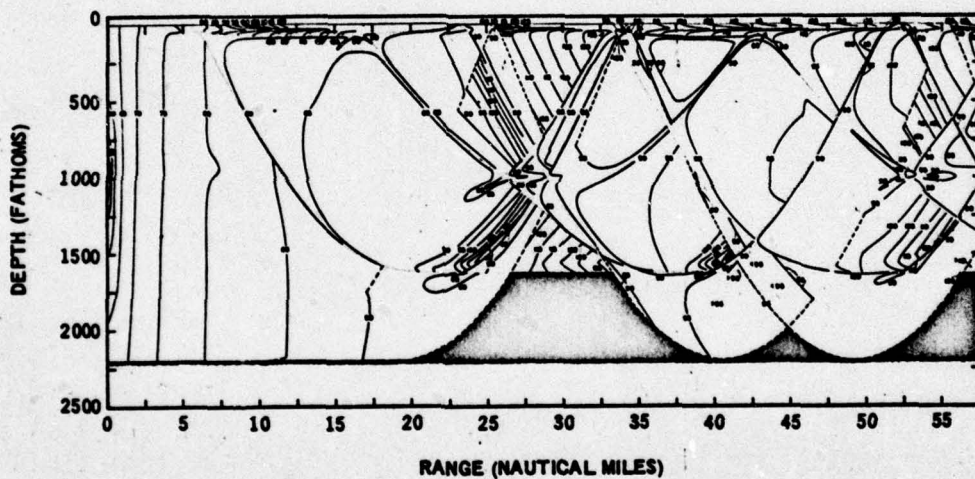


Figure 2. Propagation Loss Computed from Ray Theory

640508 0627

~~CONFIDENTIAL~~

~~CONFIDENTIAL~~

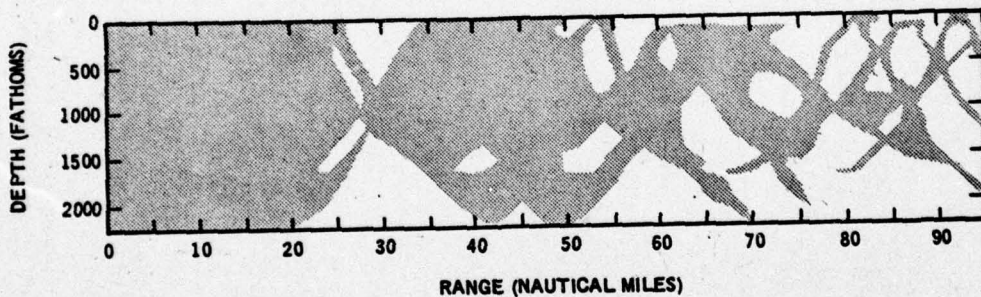


Figure 3. Propagation Loss Computed from Ray Theory

~~CONFIDENTIAL~~

~~CONFIDENTIAL~~

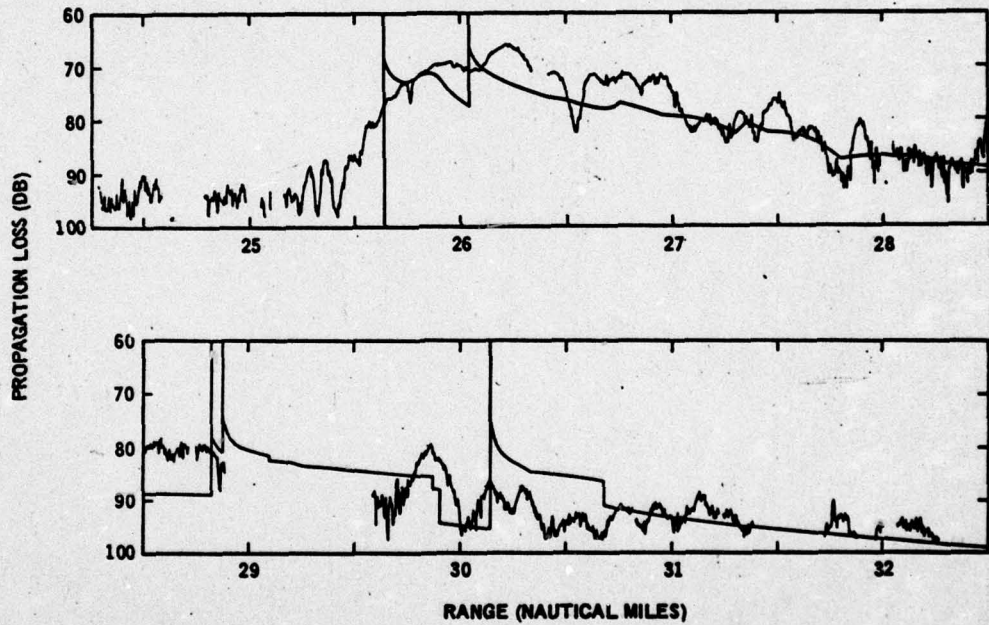


Figure 4. Experimentally Observed Propagation Loss Compared with Propagation Loss Computed from Ray Theory

~~CONFIDENTIAL~~

~~CONFIDENTIAL~~

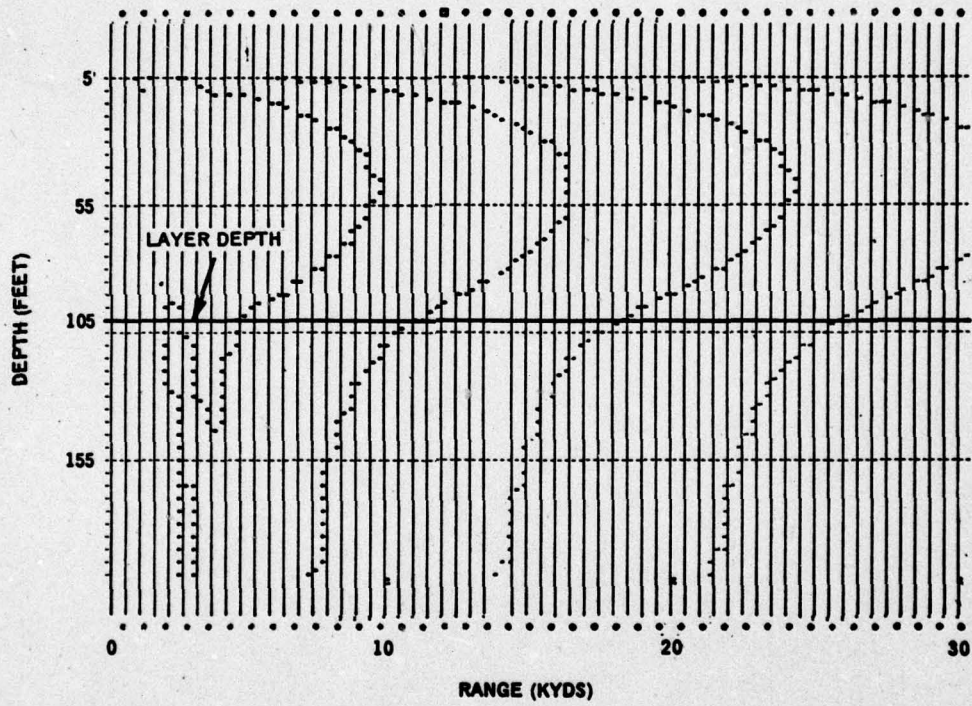


Figure 5. Propagation Loss Computed from Normal Mode Theory

640508 6627

~~CONFIDENTIAL~~

~~CONFIDENTIAL~~

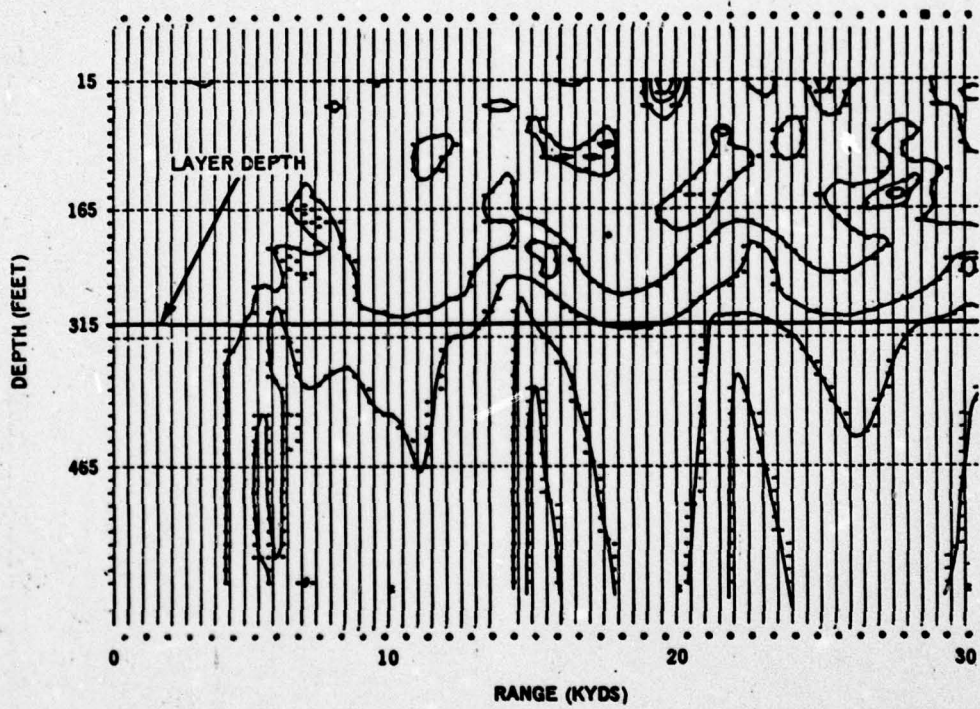


Figure 6. Propagation Loss Computed from Normal Mode Theory

~~CONFIDENTIAL~~

~~CONFIDENTIAL~~

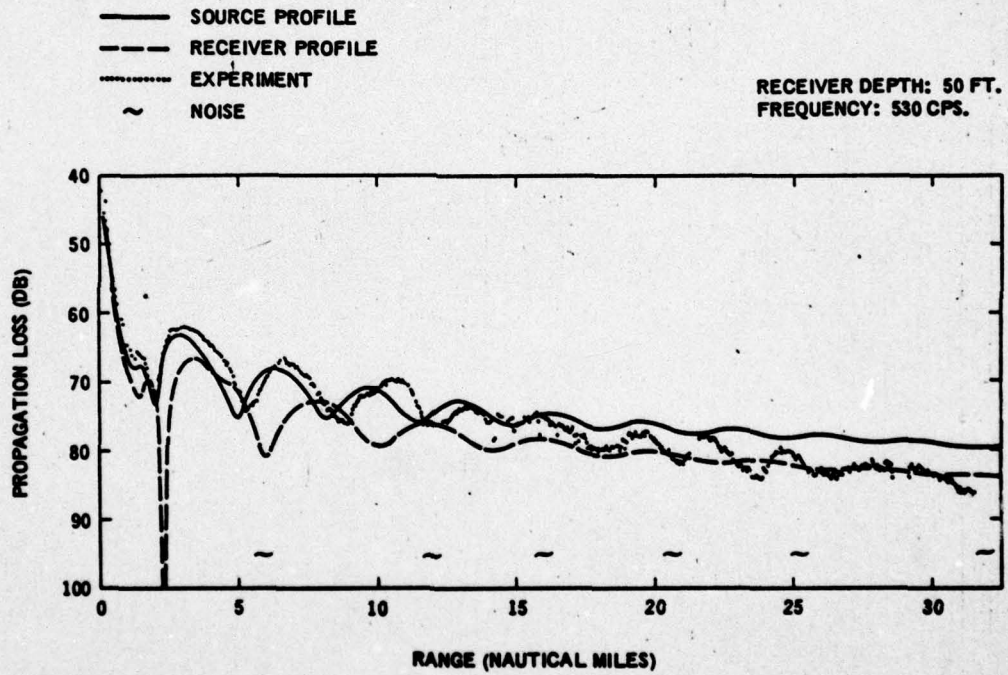


Figure 7. Experimentally Observed Propagation Loss Compared with Propagation Loss Computed from Normal Mode theory

640508 0627

~~CONFIDENTIAL~~

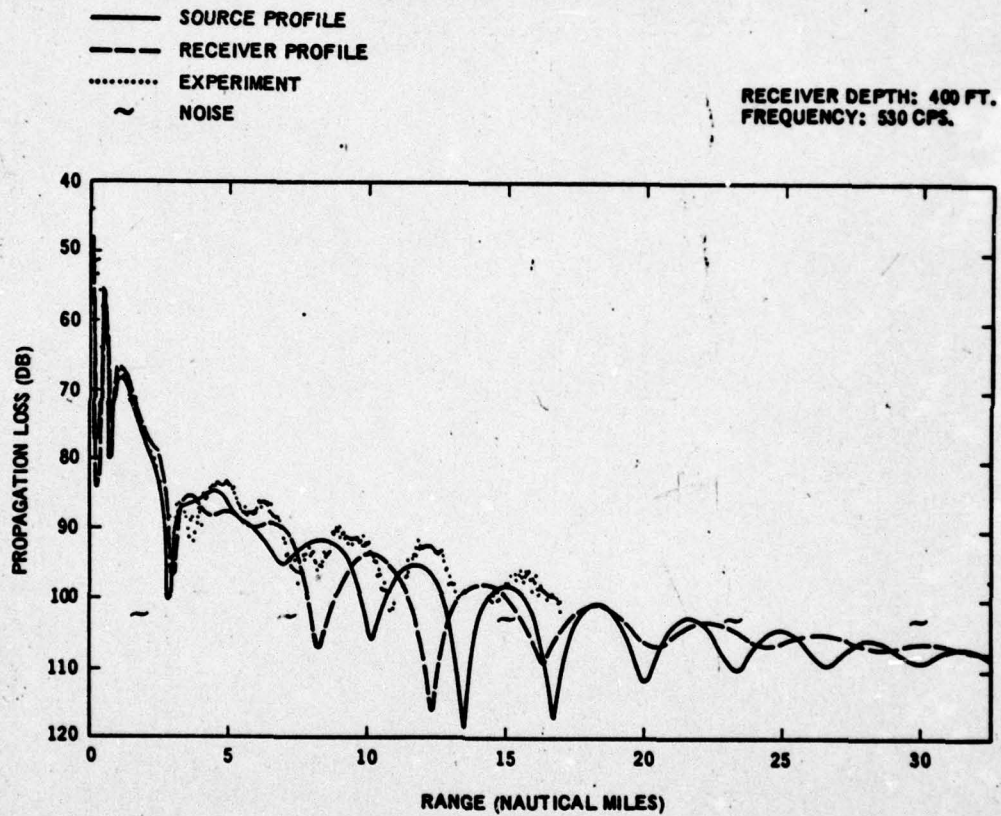


Figure 8. Experimentally Observed Propagation Loss Compared with Propagation Loss Computed from Normal Mode theory

~~CONFIDENTIAL~~

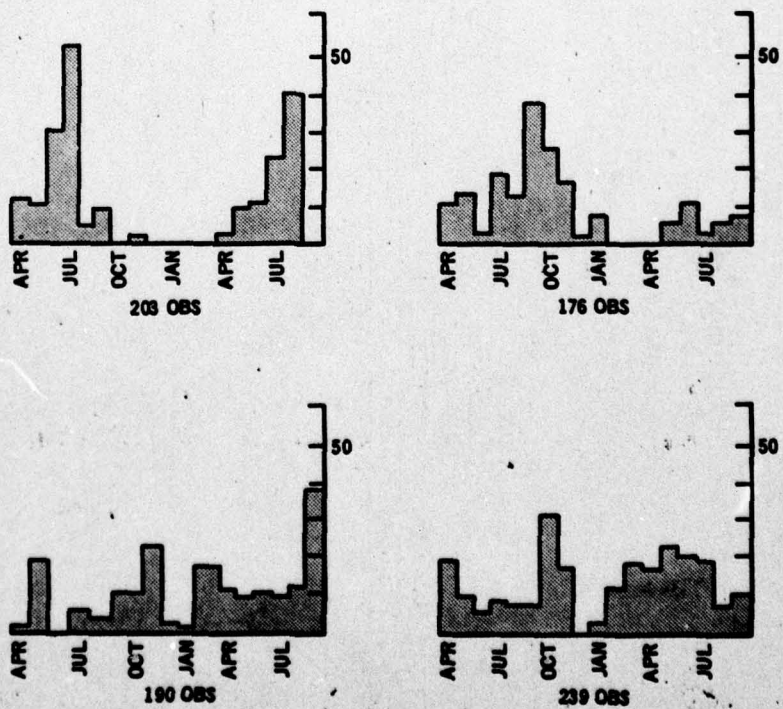
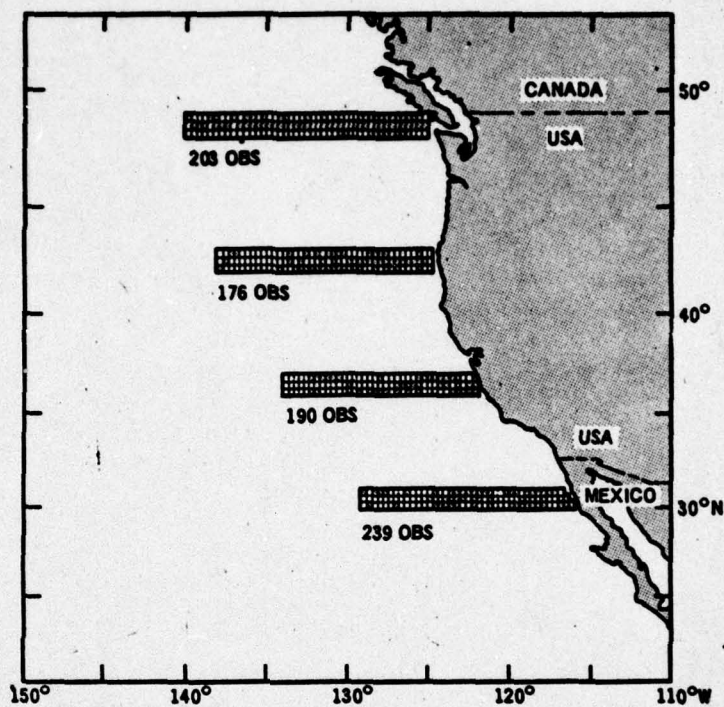


Figure 9. Distribution of Sea-Surface Temperature Data

MULTIPLE REGRESSION EQUATION

SURFACE TEMPERATURE =			
$A_0 + A_1 T + A_2 T^2 + A_3 T^3 +$	LATITUDE	T	MAIN EFFECTS
$A_4 G + A_5 G^2 + A_6 G^3 +$	LONGITUDE	G	
$A_7 D + A_8 D^2 + A_9 D^3 + A_{10} D^4 + A_{11} D^5 +$	DAY-OF-YEAR	D	
$A_{12} TD + A_{13} TD^3 + A_{14} TD^5 +$	LATITUDE x DAY OF YEAR	T x D	INTERACTIONS
$A_{15} GD + A_{16} GD^3 + A_{17} GD^5 +$	LONGITUDE x DAY OF YEAR	G x D	
$(A_{18} G + A_{19} G^2 + A_{20} G^3) T +$ $(A_{21} T^2 + A_{22} T^3) G$	LATITUDE x LONGITUDE	T x G	

Figure 10.

**STATISTICAL RESULTS OF THE
REGRESSION ANALYSIS**

NUMBER OF OBSERVATIONS	807
PERCENT VARIANCE EXPLAINED BY REGRESSION	85.7%
MULTIPLE CORRELATION COEFFICIENT	0.93
STANDARD DEVIATION OF THE OBSERVATIONS ABOUT REGRESSION	1.9°F

Figure 11.

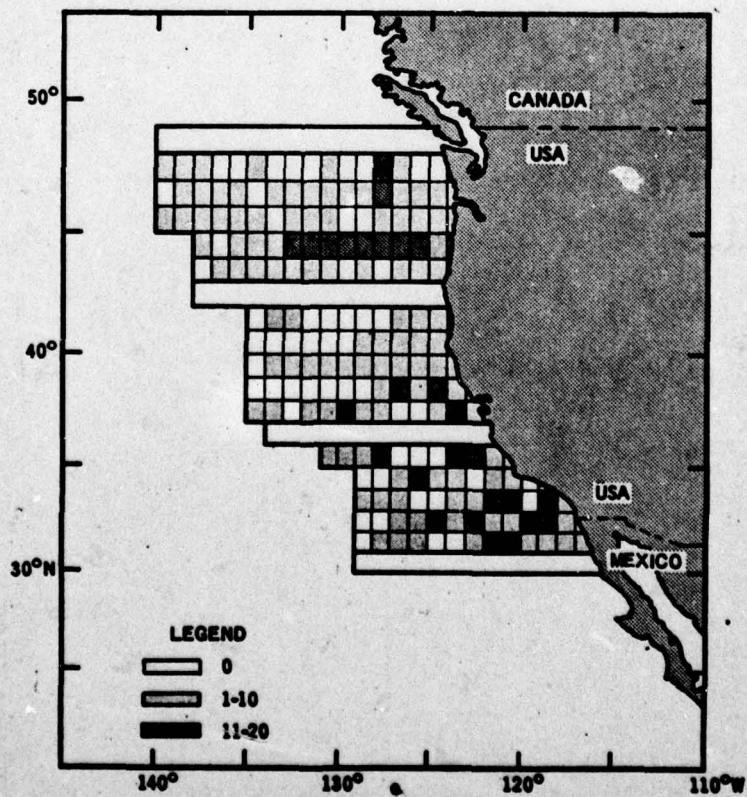
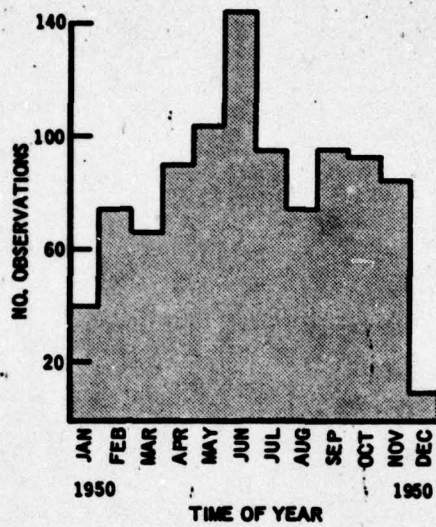


Figure 12. Location of Observations of Sea-Surface Temperature Data Used to Verify Regression Analysis

640508 0627

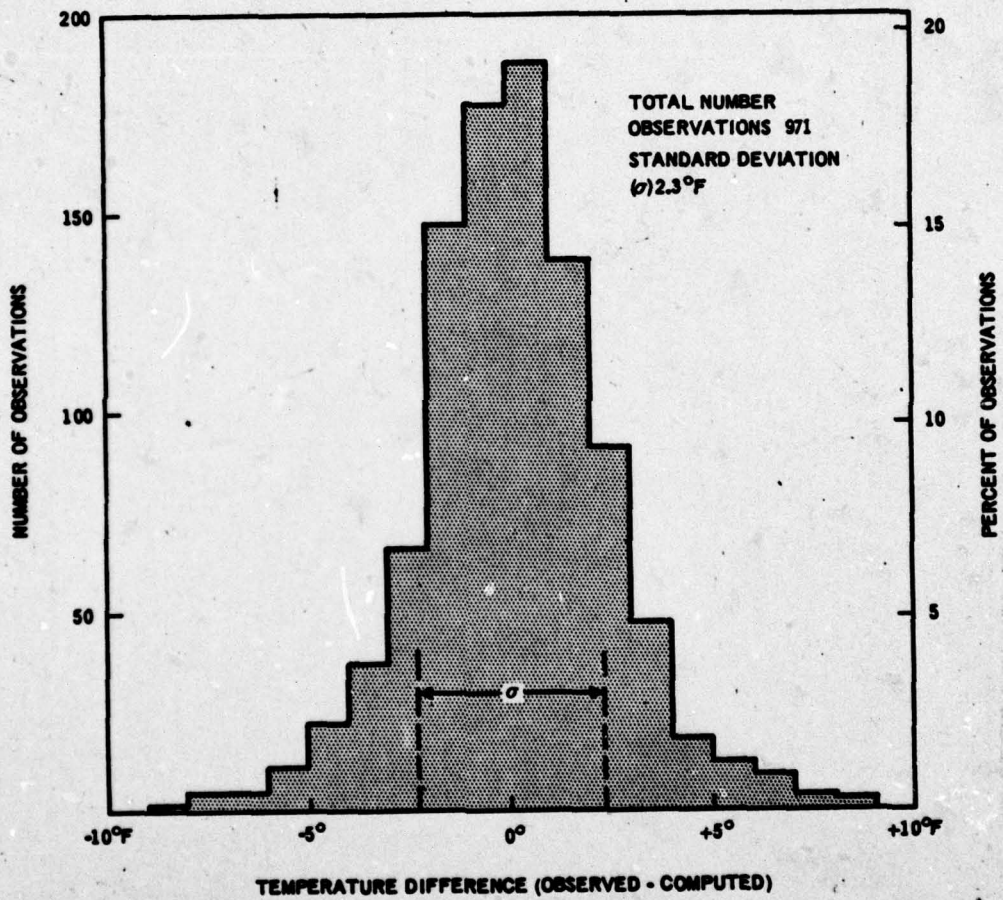


Figure 13. Histogram of Sea-Surface Temperature Differences

640508 1627

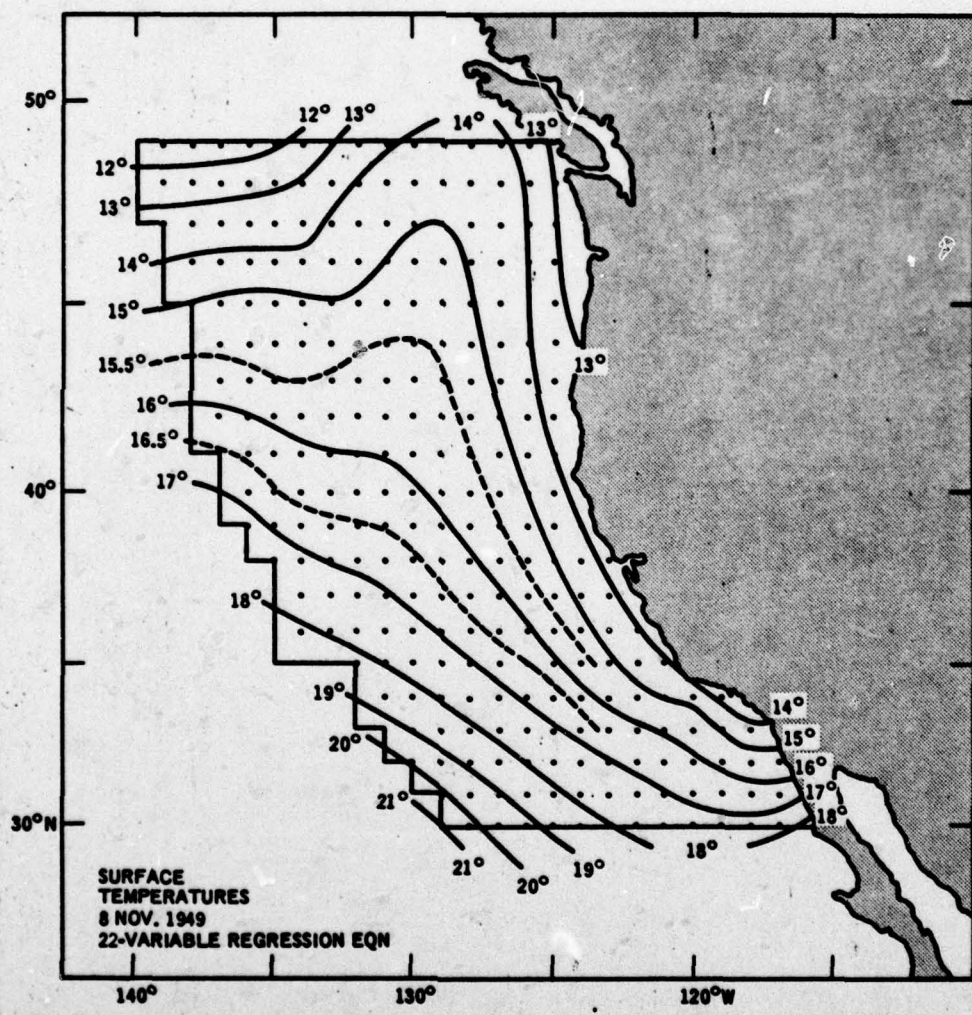


Figure 14. Sea Surface Temperature Chart

640508 0627

CONFIDENTIAL

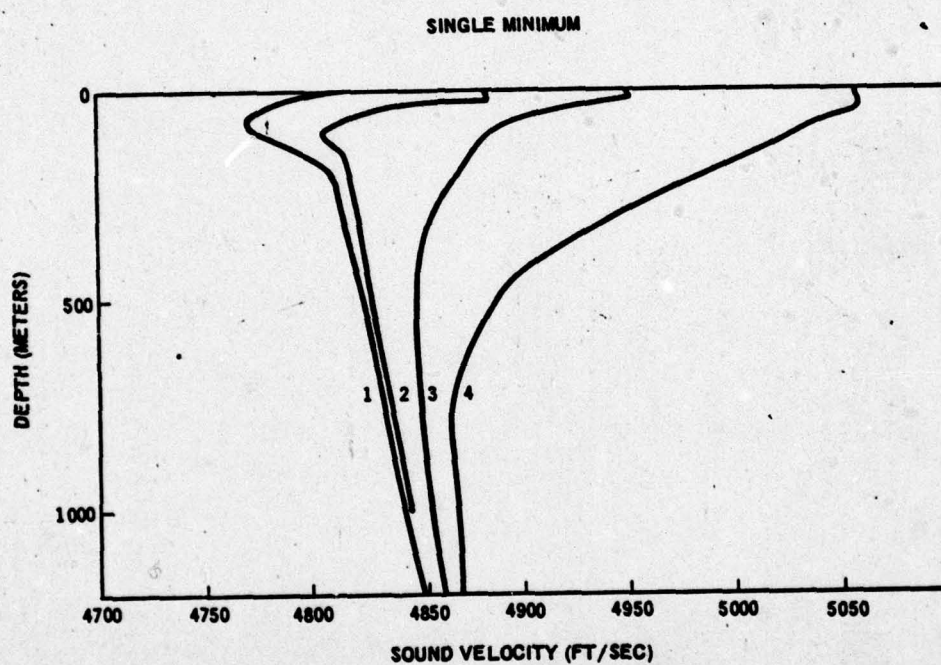


Figure 15. "Typed" Sound Velocity Profiles for the North Pacific

CONFIDENTIAL

~~CONFIDENTIAL~~

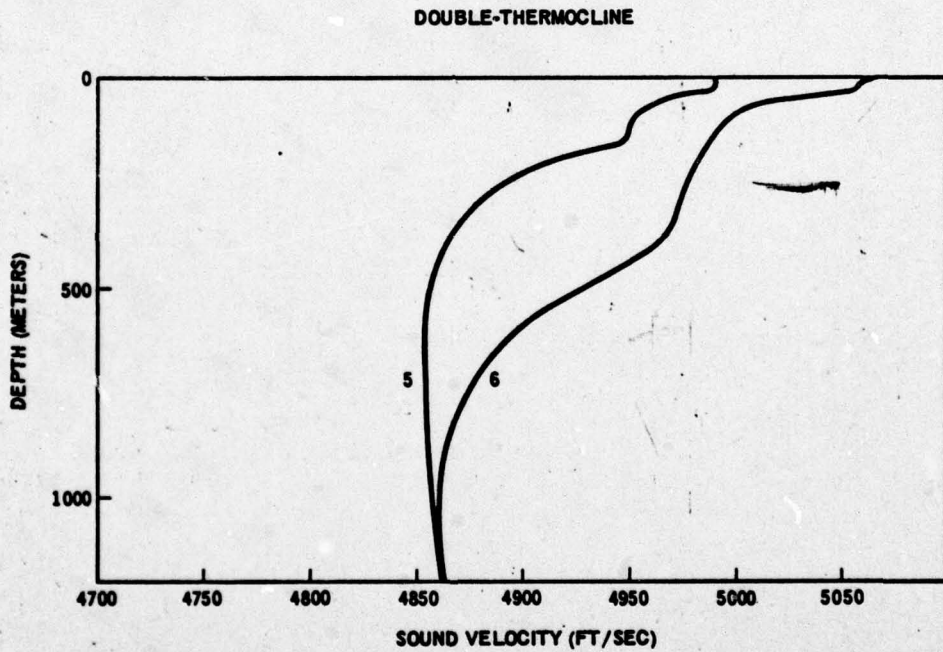


Figure 16. "Typed" Sound Velocity Profiles for the North Pacific

~~CONFIDENTIAL~~

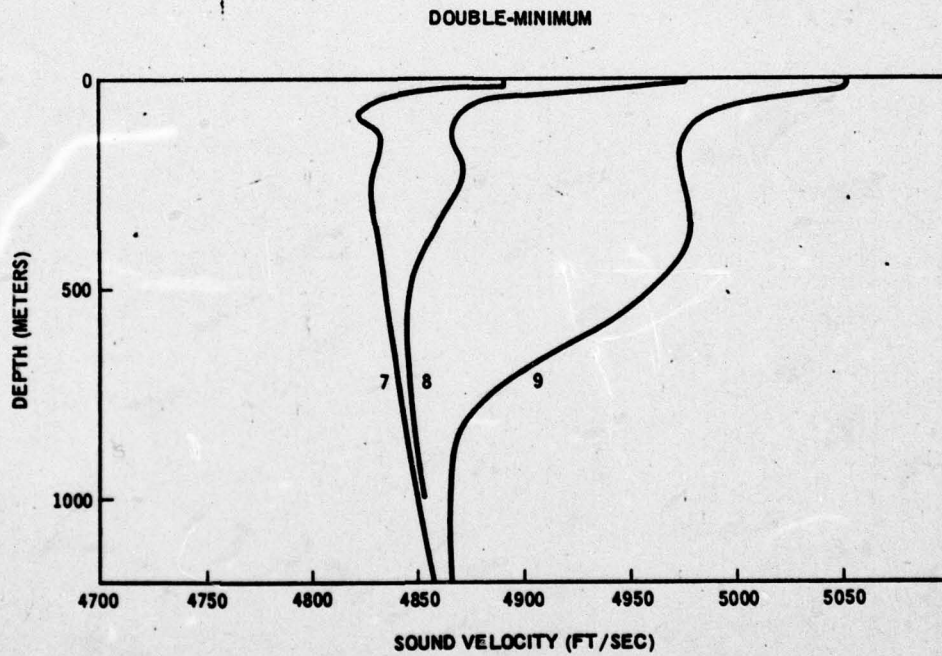


Figure 17. "Typed" Sound Velocity Profiles for the North Pacific

~~CONFIDENTIAL~~

~~CONFIDENTIAL~~

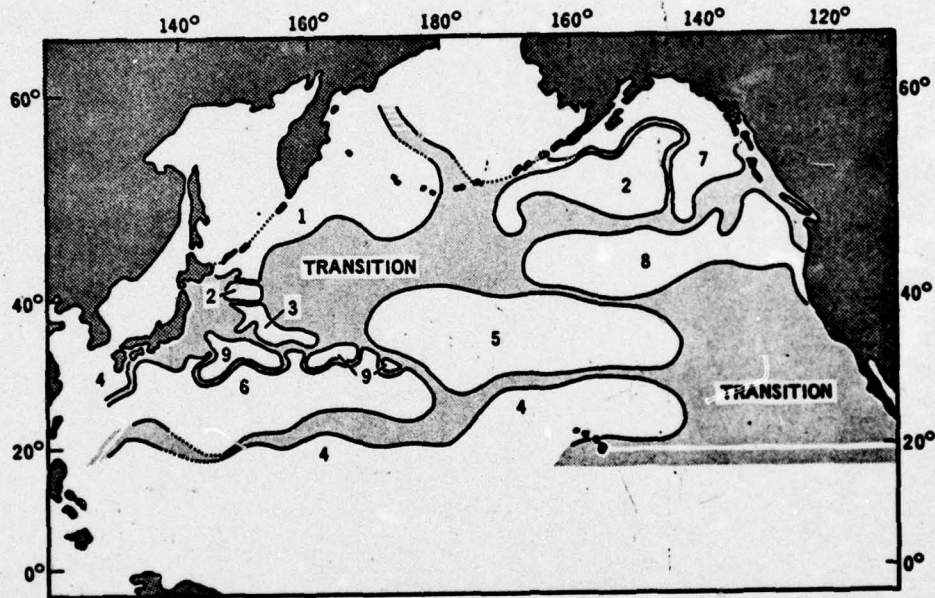


Figure 18. Location of "Typed" Volumes

~~CONFIDENTIAL~~

640508 0627

CONFIDENTIAL

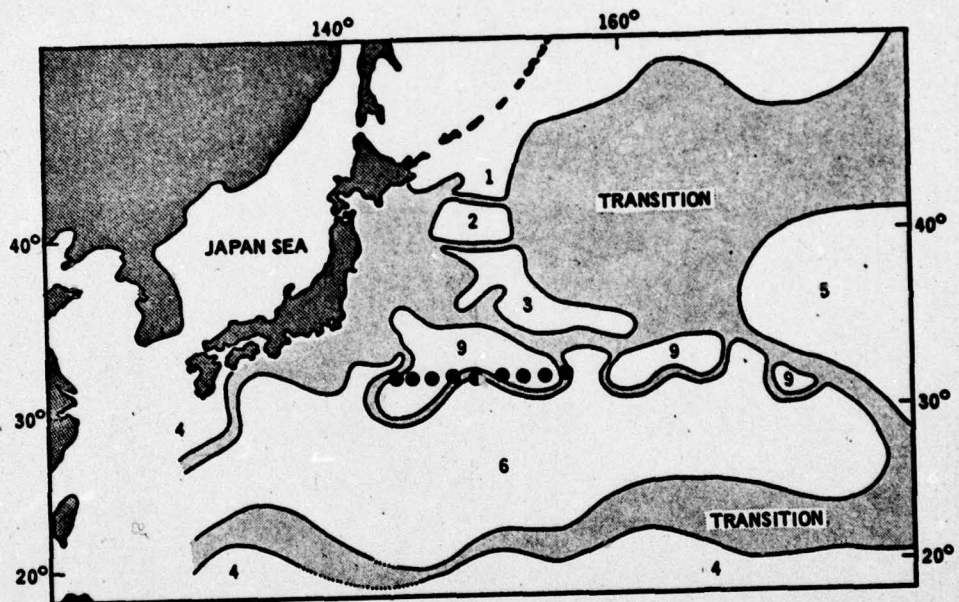


Figure 19. Location of Sound Velocity Profile Section

CONFIDENTIAL

~~CONFIDENTIAL~~

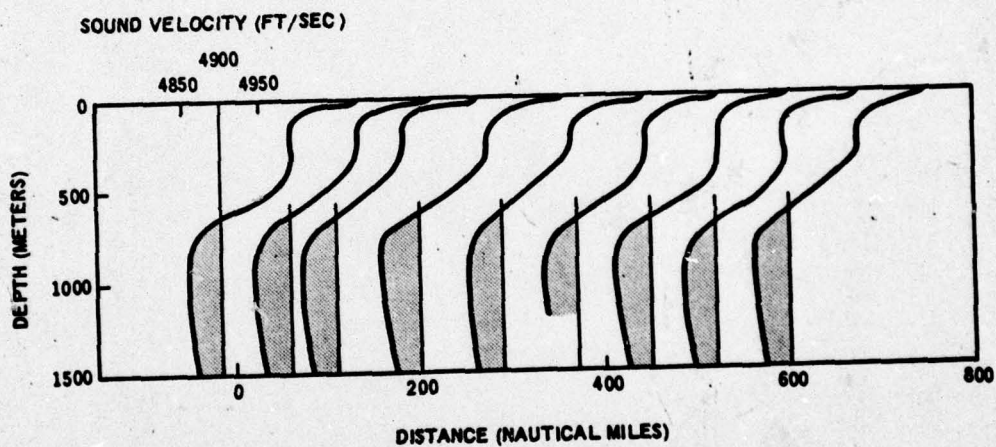


Figure 20. Sound Velocity Profiles Taken in a Homogeneous Volume

~~CONFIDENTIAL~~

640508 (627

~~CONFIDENTIAL~~

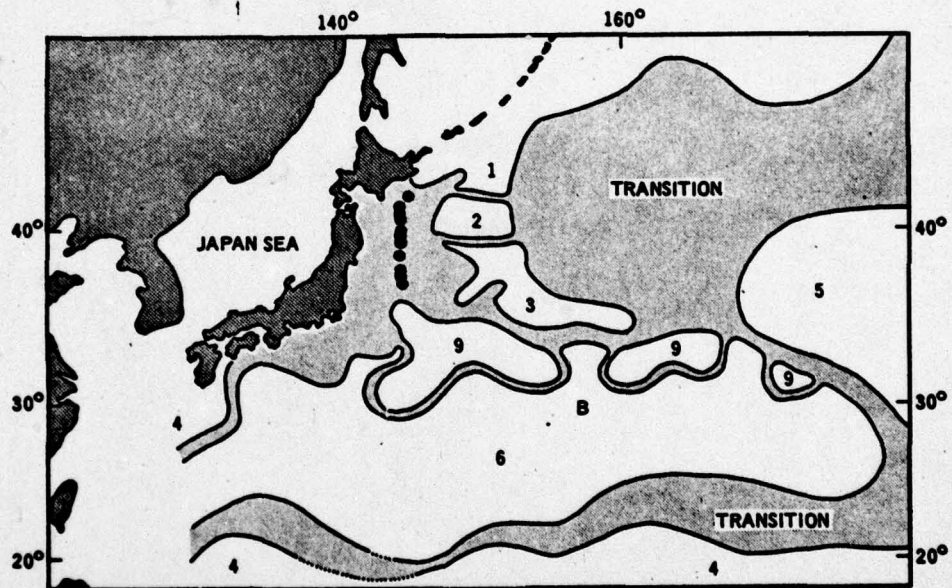


Figure 21. Location of Sound Velocity Profile Section

~~CONFIDENTIAL~~

UNCLASSIFIED

~~CONFIDENTIAL~~

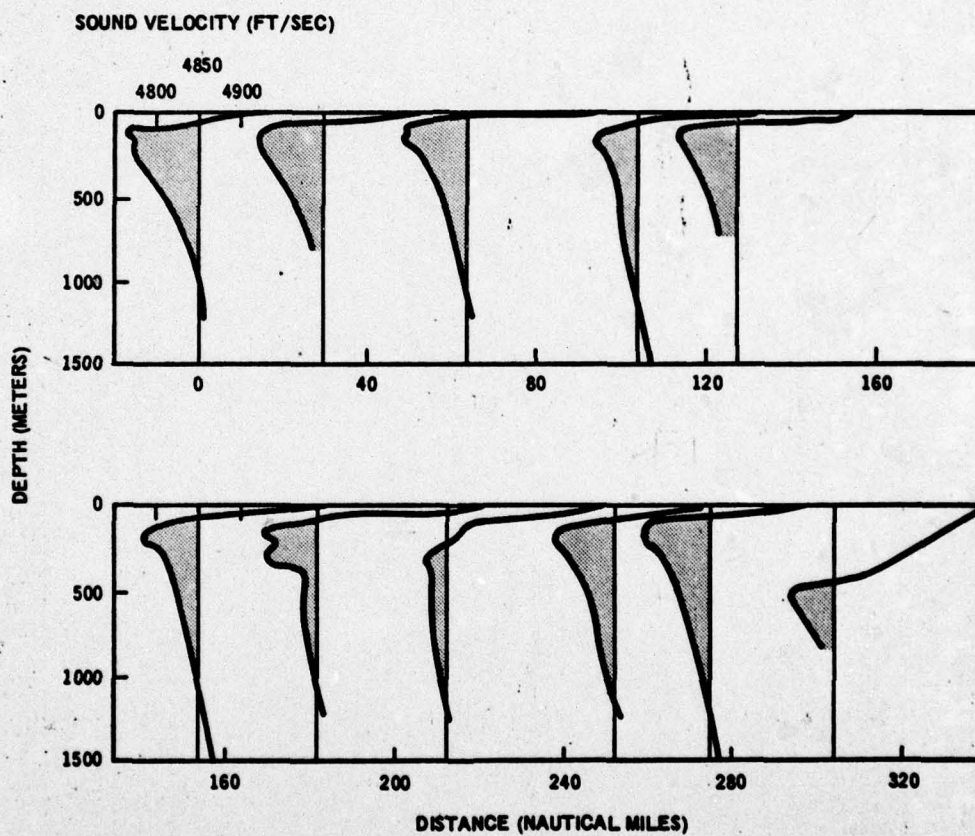


Figure 22. Sound Velocity Profiles Taken in a Transition-Volume

UNCLASSIFIED

~~CONFIDENTIAL~~

UNCLASSIFIED

UNCLASSIFIED

~~CONFIDENTIAL~~

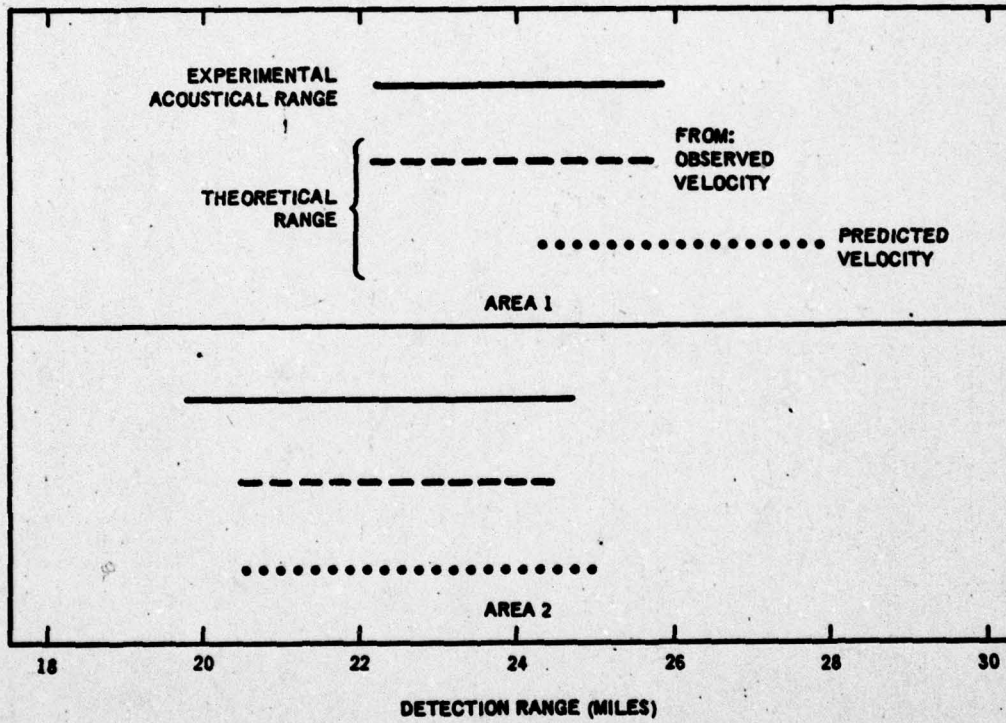


Figure 23. Experimental Verification of an Acoustic Range Prediction

UNCLASSIFIED

UNCLASSIFIED